

https://doi.org/10.1070/QEL16347

Nonlinear optical higher-order effects in an optical lattice clock

V.D. Ovsyannikov, S.I. Marmo, S.N. Mokhnenko, V.G. Pal'chikov

Abstract. **The development of optical frequency standards with a relative uncertainty of reproducing the time and frequency units at a level as low as $10^{-17}-10^{-18}$ calls for an unprecedented accuracy in estimating the role of higher orders of optical nonlinearity, caused by the influence of the optical lattice on the frequency shift of the 'clock transition'. This paper presents a systematic calculation of the contributions of multipole nonlinear anharmonic effects to the error of clocks based on optical lattices for alkaline-earth-like Sr, Yb, and Hg atoms.**

Keywords: *optical frequency standards, 'magic' wavelengths, Stark effect, polarisabilities, frequency detunings.*

1. Introduction

Currently, the so-called caesium clocks are generally accepted international standards of time and frequency. They reproduce time and frequency units based on the electron transition between the components of the hyperfine structure of caesium atom ^{133}Cs in its ground state. Today's definition of the time unit (second) in the SI system of units is related to the period of radiation corresponding to the transition between the aforementioned electron levels in the caesium atom ^{133}Cs.

The next important step in increasing the accuracy and stability of atomic clocks is the increase in the frequency of the atomic transitions in use; i.e., the passage to optical time and frequency standards, the frequency of which is several orders of magnitude higher than that of caesium microwave standards. Optical clocks can be implemented based on the transitions to the long-lived electronic states in single atoms or ions trapped into a magneto-optical trap and laser-cooled to a temperature of few microkelvins in this trap. Currently, the best results in the development of optical clocks based on cold atoms and ions have been achieved on laboratory setups in the United States (NIST), Germany (PTB), the United Kingdom (NPL), France and Japan. The following relative errors have been obtained: $\sim 10^{-18}$ for optical clocks on electron transitions in Al^+ ions placed in an electromagnetic Paul trap [1] and 2×10^{-18} for clocks based on electron transitions in neutral Sr atoms located in an optical lattice [2]. This accuracy corresponds to a lag (advance) in several fractions of a second for the lifetime of the Universe (13.7 billions of years).

Although the achievements of modern laser and spectroscopic techniques suggest a further increase in the accuracy of optical frequency and time standards, this increase meets a number of fundamental physical problems and limitations, related, in particular, to the blackbody radiation, which leads to a limit on the reproducibility and stability of the frequency of measured transitions. At the same time, the achievement of a relative error in reproducing time and frequency units at a level of $10^{-17}-10^{-18}$ in optical frequency standards calls for an unprecedented accuracy in estimating the role of higher orders of optical nonlinearity, caused by the influence of the optical lattice on the frequency shift of the 'clock transition'. One of the most successful approaches to the solution of this important problem is the use of the so-called magic wavelength (MWL) of the laser field forming the optical lattice in a frequency standard.

The magic wavelength of the optical lattice that is used to trap cold alkaline-earth-like atoms in the Lamb–Dicke regime, allows one to observe a clock transition between the ground $6s^2(^1S_0)$ and excited metastable $6s6p(^3P_0)$ states of atoms free of Doppler and Stark frequency shifts. The experimental MWL values for strontium, ytterbium and mercury atoms were found to be $\lambda_{mag} = 813.42727$ nm for Sr atoms [3], $\lambda_{mag} = 759.3537$ nm for Yb atoms [4] and $\lambda_{mag} = 362.53$ nm for Hg atoms [5]. In the case of the MWL, the dynamic Stark effect in atoms in the ground and excited states leads to the same field corrections for these states, which, in turn, provides their complete mutual compensation in the clock transition of the optical frequency standard. However, the equivalence of Stark frequency shifts, which are linear in the lattice field intensity I and determined by the dynamic polarisabilities $\alpha_e(\omega_{mag}) = \alpha_g(\omega_{mag})$ at the MWL $\lambda_{mag} = 2\pi c/\omega_{mag}$, does not ensure equivalent contributions from higher-order nonlinearities, primarily, the corrections quadratic in intensity I, which are determined by the hyperpolarisabilities $\beta_e(\omega_{mag})$ and $\beta_g(\omega_{mag})$.

In addition, along with the dipole polarisabilities $\alpha^{E1}_{e(g)}(\omega_{mag})$ (E1), there are higher-order multipole polarisabilities, primarily, the magnetic dipole, $\alpha^{M1}_{e(g)}(\omega_{mag})$ (M1), and electric quadrupole, $\alpha^{E2}_{e(g)}(\omega_{mag})$ (E2), polarisabilities of atomic states, which make a nonzero contribution to the dynamic Stark effect (linear in intensity I). The correction caused by the multipole interactions, although having an order of smallness of $\sim 10^{-6}-10^{-7}$ with respect to the electric dipole approximation (E1), leads to a peculiar spatial field distribution in the lattice, which significantly differs from that in the case of E1 approximation;

V.D. Ovsyannikov, S.I. Marmo, S.N. Mokhnenko Voronezh State University, Universitetskaya pl. 1, 394006 Voronezh, Russia; e-mail: ovd@phys.vsu.ru;
V.G. Pal'chikov All-Russian Research Institute of Physicotechnical and Radiotechnical Measurements, 141570 Mendeleevo, Moscow region, Russia; National Research Nuclear University 'MEPhI', Kashirskoe sh. 31, 115409 Moscow, Russia; e-mail: vitpal@mail.ru

Received 9 March 2017
Kvantovaya Elektronika **47** (5) 412–420 (2017)
Translated by Yu.P. Sin'kov

hence, it must be correctly taken into account in precise frequency measurements. In particular, the corrections for the E2 and M1 approximations may affect the MWL, depending on the specific experimental conditions. For example, the Stark shift (linear in intensity I) in the travelling wave, which is characterised by a uniform spatial distribution of field intensity along the laser beam axis, is determined by the sum of the polarisabilities

$$\alpha^{\Sigma}_{e(g)}(\omega^{t}_{mag}) = \alpha^{E1}_{e(g)}(\omega^{t}_{mag}) + \alpha^{qm}_{e(g)}(\omega^{t}_{mag}),$$

where $\alpha^{qm}_{e(g)}(\omega^{t}_{mag}) = \alpha^{E2}_{e(g)}(\omega^{t}_{mag}) + \alpha^{M1}_{e(g)}(\omega^{t}_{mag})$ is the sum of the E2 and M1 polarisabilities. However, in the standing wave of the optical lattice, the E2 and M1 polarisabilities lag in phase by a quarter wave from the E1 polarisability. Hence, they must be subtracted from the E1 polarisability; i.e., $\alpha^{dqm}_{e(g)}(\omega^{s}_{mag}) = \alpha^{E1}_{e(g)}(\omega^{s}_{mag}) - \alpha^{qm}_{e(g)}(\omega^{s}_{mag})$ and the MWL $\lambda^{t(s)}_{mag} = 2\pi c/\omega^{t(s)}_{mag}$ is determined differently for the travelling and standing waves of the optical lattice:

$$\alpha^{\Sigma}_{e}(\omega^{t}_{mag}) = \alpha^{\Sigma}_{g}(\omega^{t}_{mag}) \tag{1}$$

for the travelling wave and

$$\alpha^{dqm}_{e}(\omega^{s}_{mag}) = \alpha^{dqm}_{g}(\omega^{s}_{mag}) \tag{2}$$

for the standing wave [6]. It should be noted that the measurement of the difference in the two MWLs, λ^{t}_{mag} and λ^{s}_{mag}, is in principle within the possibilities of a modern experiment based on the use of laser lattices. Nevertheless, as will be shown below, even the minimum MWL detuning can be used to control the contribution of the higher-order effects to the error of optical frequency and time standards. Up to recent time, this analysis has not been performed in the metrological practice.

There are two main types of the MWL, corresponding to two different ways of trapping cold atoms: (1) the use of an attractive potential in the trap, for which the potential energy of atoms has a minimum, and the trapped atoms are located in the vicinities of laser lattice antinodes (red-detuned MWL) and (2) the use of a repulsive potential in the trap, in which the atoms are located in the vicinities of laser lattice nodes where $I = 0$ (blue-detuned MWL). Obviously, in the latter case, the role of higher-order effects may be significantly reduced in comparison with the case of red detuning. However, the blue MWL detuning calls for a three-dimensional modification of the optical lattice design, because its one-dimensional modification can hardly be implemented in view of the properties of the repulsive potential. In this paper, we will consider both optical lattice versions for the one-dimensional case in order to analyse and estimate the role of 'nonmagic' effects and elaborate possible strategies when developing optical frequency standards based on optical lattices.

The most thoroughly investigated version of optical clocks based on Sr atoms was described in detail in our recent paper [6]. The analysis was performed in the basis of the Fues model potential (FMP) as applied to the calculation of atomic polarisabilities and hyperpolarisabilities [7]. In this study, we calculated anew the atomic characteristics reported in [6]; this new calculation is based on redetermination of the FMP parameters. The quality criterion for choosing the FMP parameters was the goodness of fit between the theoretically calculated and experimental MWLs for the alkaline-earth-like Sr, Yb and Hg atoms.

Three different strategies for determining MWLs are considered for each of the Sr, Yb and Hg atoms. In addition to the MWL definitions given by formulas (1) and (2), we consider the intermediate case of equivalence of only dipole polarisabilities for the ground and excited states:

$$\alpha^{E1}_{e}(\omega^{d}_{mag}) = \alpha^{E1}_{g}(\omega^{d}_{mag}). \tag{3}$$

The MWL definition (3) is most frequently used in the modern literature. As was noted for the first time in [6], the influence of multipole effects may lead to additional contributions to the error of optical time and frequency standards, even when the effects of spatial distribution for electric dipole and multipole interactions in the optical lattice field are disregarded.

In this paper, we report the results of careful analysis of the difference in the spatial distributions for electric dipole (E1) and multipole (M1 and E2) interactions for two configurations of optical lattices with MWL red and blue detunings. For brevity, we consider only the particular case of a one-dimensional optical lattice. The results of theoretical calculations for the frequency shifts of transitions in Sr, Yb and Hg atoms in an optical lattice are presented. A precise estimation is performed for the contributions of nonlinear optical higher-order effects, which cannot be compensated for by choosing an appropriate MWL and, therefore, must be correctly taken into account when analysing the results of measuring the clock transition frequency in optical frequency standards. We applied the atomic system of units, where the condition $e = m = \hbar = 1$ holds.

2. Optical lattices in the case of MWL red detuning

The frequency shift induced by the lattice laser field arises as a difference in the Stark energies for the ground and excited states of the clock transition. The Stark energies are determined from the interaction of the atom in the trap with the electric field vector

$$\boldsymbol{E}(X,t) = 2\boldsymbol{E}_0 \cos(kX)\cos(\omega t), \tag{4}$$

which oscillates in time with a frequency ω and propagates in space with a wave vector $\boldsymbol{k} = k\boldsymbol{e}_x$ ($k = \omega/c$); X is the displacement of an atom from the equilibrium position in the laser lattice. The interaction between the atom and lattice is described by the operator $\hat{V}(X,t) = \mathrm{Re}[\hat{V}(X)\exp(-i\omega t)]$; the spatial factor is given by the expression

$$\hat{V}(X) = \hat{V}_{E1}\cos(kX) + (\hat{V}_{E2} + \hat{V}_{M1})\sin(kX) \tag{5}$$

and the operators of the E1, E2 and M1 interactions have the form

$$\begin{aligned} &\hat{V}_{E1} = \boldsymbol{r}\boldsymbol{E}_0, \quad \hat{V}_{E2} = \frac{\alpha\omega}{\sqrt{6}}\, r^2(\{\boldsymbol{E}_0 \otimes \boldsymbol{n}\}_2\, \boldsymbol{C}_2(\theta,\varphi)), \\ &\hat{V}_{M1} = \frac{\alpha}{2}\{[\boldsymbol{n}\times\boldsymbol{E}_0](\hat{\boldsymbol{J}} + \hat{\boldsymbol{S}})\}. \end{aligned} \tag{6}$$

Here, $\boldsymbol{r} = r\boldsymbol{n}$ is the radius vector of the valence electron; $\boldsymbol{C}_2(\theta,\varphi)$ is the modified spherical harmonic of the unit vector $\boldsymbol{n}$ for the angular variables θ and φ; and $\hat{\boldsymbol{J}}$ and $\hat{\boldsymbol{S}}$ are, respec-

tively, the total and spin moments of the atom. With allowance for the second- and fourth-order terms in the interaction of atoms with the lattice field (which are linear and quadratic in the lattice field intensity I [8]), formulas (6) determine the lattice potential well U [6] in the ground or excited state:

$$U^{\rm latt}_{\rm g(e)}(X,I) \approx -D_{\rm g(e)}(I) + U^{\rm harm}_{\rm g(e)}(I)X^2 - U^{\rm anh}_{\rm g(e)}(I)X^4 + ..., \quad (7)$$

where the potential energy is counted from its lowest value $U^{\rm latt}_{\rm g(e)}(0,I) = -D_{\rm g(e)}(I)$; the well depth

$$D_{\rm g(e)}(I) = \alpha^{\rm E1}_{\rm g(e)}(\omega)I + \beta_{\rm g(e)}(\omega)I^2 \quad (8)$$

is determined by the electric dipole polarisabilities $\alpha^{\rm E1}_{\rm g(e)}(\omega)$ and hyperpolarisabilities $\beta_{\rm g(e)}(\omega)$ of atoms in the ground or excited state. The coefficient before the squared displacement,

$$U^{\rm harm}_{\rm g(e)}(I) = \left[\alpha^{\rm dqm}_{\rm g(e)}(\omega)I + 2\beta_{\rm g(e)}(\omega)I^2\right]k^2 = \frac{M\Omega^2_{\rm g(e)}(I)}{2}, \quad (9)$$

where M is the atomic mass, is determined by the intensity-dependent oscillation eigenfrequency $\Omega_{\rm g(e)}(I)$ for the ground and excited states of the atom in the potential well (7). The coefficient before the fourth power of X depends on the lowest anharmonic correction to the Stark potential in the standing wave of the lattice and on the combinations of the E1, E2, and M1 polarisabilities $\alpha^{\rm dqm}_{\rm g(e)}(\omega) = \alpha^{\rm E1}_{\rm g(e)}(\omega) - \alpha^{\rm qm}_{\rm g(e)}(\omega)$ and hyperpolarisabilities, in correspondence with the formula

$$U^{\rm anh}_{\rm g(e)}(I) = \left[\alpha^{\rm dqm}_{\rm g(e)}(\omega)I + 5\beta_{\rm g(e)}(\omega)I^2\right]\frac{k^4}{3}. \quad (10)$$

Equation (7) describes the lattice potential in the spatial region $|X| \ll \lambda/4$, where λ is the lattice laser field wavelength; the atoms in the lattice are located with a spatial periodicity of $\lambda/2$. An atom trapped into the laser lattice continues an oscillatory motion in the stationary state with the energy

$$\mathcal{E}^{\rm vib}_{\rm g(e)}(I,n) = -D_{\rm g(e)}(I) + \Omega_{\rm g(e)}(I)\left(n + \frac{1}{2}\right) - \mathcal{E}^{\rm anh}_{\rm g(e)}(I)\left(n^2 + n + \frac{1}{2}\right), \quad (11)$$

where the second term is the harmonic oscillator energy in the state with the principal vibrational quantum number n, and the third term takes into account the anharmonic corrections caused by the last term in the expression for the potential energy (7). Thus, the frequency shift induced by the lattice field arises as a difference in the oscillator energies (11) of the atom in the ground and excited states. On the assumption that the principal vibrational quantum numbers n are equivalent for the transitions between the states of the clock transition (the Lamb–Dicke regime), the frequency shift of this transition is given by the expression

$$\Delta\nu^{\rm latt}_{\rm cl}(I,n) = \mathcal{E}^{\rm vib}_{\rm e}(I,n) - \mathcal{E}^{\rm vib}_{\rm g}(I,n) = -\Delta D(I) + \Delta\Omega(I)\left(n + \frac{1}{2}\right) - \Delta\mathcal{E}^{\rm anh}(I)\left(n^2 + n + \frac{1}{2}\right), \quad (12)$$

where

$$\Delta D(I) = D_{\rm e}(I) - D_{\rm g}(I); \quad \Delta\Omega(I) = \Omega_{\rm e}(I) - \Omega_{\rm g}(I); \quad \Delta\mathcal{E}^{\rm anh}(I) = \mathcal{E}^{\rm anh}_{\rm e}(I) - \mathcal{E}^{\rm anh}_{\rm g}(I). \quad (13)$$

The differences in (13) correspond to:

(1) the potential well depths (8);

(2) harmonic-oscillation frequencies of the atom in the potential (7),

$$\Omega_{\rm g(e)}(I) = 2\sqrt{\mathcal{E}^{\rm rec}\left[\alpha^{\rm dqm}_{\rm g(e)}(\omega)I + 2\beta_{\rm g(e)}(\xi,\omega)I^2\right]}, \quad (14)$$

which are determined by the photon recoil energies $\mathcal{E}^{\rm rec} = k^2/(2M)$ and the coefficient (9) of the harmonic part of potential (7) [ξ is the degree of circular polarisation ($-1 \leqslant \xi \leqslant 1$)]; and

(3) the anharmonic corrections to the atomic vibrations in a trap with separated potential wells of the optical lattice,

$$\mathcal{E}^{\rm anh}_{\rm g(e)}(I) = \frac{\mathcal{E}^{\rm rec}}{2}\left[1 + \frac{3\beta_{\rm g(e)}(\xi,\omega)I}{\alpha^{\rm dqm}_{\rm g(e)}(\omega)}\right], \quad (15)$$

which correspond to the last term in the right-hand side of formula (7).

The difference of the dipole and multipole polarisabilities $\alpha^{\rm dqm}_{\rm g(e)}(\omega)$ (instead of the sum $\alpha^{\Sigma}_{\rm g(e)}(\omega) = \alpha^{\rm E1}_{\rm g(e)}(\omega) + \alpha^{\rm qm}_{\rm g(e)}(\omega)$, which arises in the case of interaction between the atom and the travelling wave of the optical lattice) is due to the shift by a quarter period (both for the temporal and spatial variables) between the E1 and (E2 + M1) polarisabilities of the atom interacting with the standing wave of the optical lattice [9]. As follows from Eqns (8)–(15), the intensity-dependent energy differences, determining the frequency shift (12), have the form [6]

$$\Delta D = [\alpha^{\rm E1}_{\rm e}(\omega) - \alpha^{\rm E1}_{\rm g}(\omega)]I + [\beta_{\rm e}(\xi,\omega) - \beta_{\rm g}(\xi,\omega)]I^2,$$

$$\Delta\Omega = 2\left[\sqrt{\alpha^{\rm dqm}_{\rm e}(\omega) + 2\beta_{\rm e}(\xi,\omega)I} - \sqrt{\alpha^{\rm dqm}_{\rm g}(\omega) + 2\beta_{\rm g}(\xi,\omega)I}\right]\sqrt{\mathcal{E}^{\rm rec}I},$$

$$\Delta\mathcal{E}^{\rm anh} = \frac{3}{2}\mathcal{E}^{\rm rec}\left[\frac{\beta_{\rm e}(\xi,\omega)}{\alpha^{\rm dqm}_{\rm e}(\omega)} - \frac{\beta_{\rm g}(\xi,\omega)}{\alpha^{\rm dqm}_{\rm g}(\omega)}\right]I. \quad (16)$$

Finally, the lattice-field-induced frequency shift of the clock transition, with allowance for the corrections quadratic in the field intensity I, can be written as

$$\Delta\nu^{\rm latt}_{\rm cl}(n,\xi,I) = c_{1/2}(n)I^{1/2} + c_1({\rm n},\xi)I + c_{3/2}(n,\xi)I^{3/2} + c_2(\xi)I^2. \quad (17)$$

Having performed frequency detuning for the laser lattice field in the vicinity of the MWL, one can minimise the field-intensity-independent coefficients c_i (i = 1/2, 1, 3/2, and 2). The fractional exponents of intensity I in formula (17) are due to the root dependence of the eigenfrequencies (14) on I. In particular, the coefficient $c_{1/2}$ is determined by the difference in the combinations of polarisabilities $\alpha^{\rm dqm}_{\rm g(e)}(\omega)$. The term linear in I depends mainly on the difference in the dielectric dipole polarisabilities $\alpha^{\rm E1}_{\rm g(e)}(\omega)$ [the hyperpolarisability correction for the term linear in I (having a much smaller amplitude) is due to the anharmonic correction in (16)]. The coefficients $c_{3/2}$ and c_2 depend on the difference in the hyperpolarisabilities $\Delta\beta(\xi,\omega) = \beta_{\rm e}(\xi,\omega) - \beta_{\rm g}(\xi,\omega)$, entering the formulas for the eigenfrequencies $\Omega_{\rm g(e)}$ and potential well depths $D_{\rm g(e)}$. Along

Table 1. Characteristics of the Sr, Yb and Hg atoms in an optical lattice of the MWL.

Atom	λ_{mag}/nm	α^{E1}_{mag}/ kHz / kW cm^{-2}	α^{qm}_{mag}/ mHz / kW cm^{-2}	Re $\Delta\beta^{lin}_{mag}$/ μHz / (kW cm^{-2})^2	Im $\Delta\beta^{lin}_{mag}$/ μHz / (kW cm^{-2})^2	Re $\Delta\beta^{circ}_{mag}$/ μHz / (kW cm^{-2})^2	Im $\Delta\beta^{circ}_{mag}$/ μHz / (kW cm^{-2})^2	$\Omega_{mag}/\sqrt{T}$/ kHz / $\sqrt{\text{kW cm}^{-2}}$	$10^9\partial(\Delta\alpha^{E1}_{mag})/\partial\omega$/ 1 / kW cm^{-2}	$\mathcal{E}^{rec}$/ kHz
Sr	813.42727	45.2	1.38	–200.0	0	–311.0	0	25.05	0.254	3.47
	389.889	–92.7	–13.6	1150	2.48	1550	2.37	74.8	10.3	15.1
Yb	759.3537	40.5	–8.06	–366.3	0	240.2	0	18.03	0.720	2.00
Hg	362.53	5.70	8.25	–2.50	4.34	2.53	6.37	13.1	0.134	7.57

with the dependence on the laser lattice frequency, hyperpolarisabilities depend also on the polarisations of the lattice field [10]. This dependence can be written as a combination of the hyperpolarisability tensor components:

$$\beta_{g(e)}(\omega,\xi) = \beta^{lin}_{g(e)}(\omega) + \xi^2\left[\beta^{circ}_{g(e)}(\omega) - \beta^{lin}_{g(e)}(\omega)\right], \qquad (18)$$

where $\beta^{lin(circ)}_{g(e)}(\omega)$ is the frequency-dependent hyperpolarisability for the linear (circular) polarisation of the laser lattice field.

The $\Delta\beta^{lin}$ and $\Delta\beta^{circ}$ values have opposite signs when there is a 'magic degree of circular polarisation', $\xi_{mag} = \pm 1/\sqrt{1 - \Delta\beta^{circ}/\Delta\beta^{lin}}$, at which the difference in the hyperpolarisabilities for the clock transition in (18) may vanish. This effect, as follows from Table 1 (which contains the characteristics of Sr, Yb and Hg atoms calculated within the model potential approximation [7]) can be observed for the MWL in Yb atoms at $\xi_{mag} = 0.777$ and in Hg atoms at $\xi_{mag} = 0.705$. For Sr atoms, the differences $\Delta\beta^{lin}_{mag}$ and $\Delta\beta^{circ}_{mag}$ at the MWL are negative; thus, the magic ellipticity does not exist in this case, and the minimum difference in the hyperpolarisabilities corresponds to linear polarisation. The additional row for strontium atoms in Table 1 corresponds to the MWL with blue detuning $\lambda_{mag} = 389.889$ nm [11].

Magic ellipticity can be observed for Yb atoms at lattice wavelengths in the range of $758.5 < \lambda_{latt} < 759.7$ nm, which is close to the region of two-photon resonance at the 6s8p(^{3}P$_0$) level for a linearly polarised lattice wave (Fig. 1); this region corresponds to the MWL $\lambda_{mag} = 759.3537$ nm [4]. Here, the hyperpolarisability differences $\Delta\beta^{lin}$ and $\Delta\beta^{circ}$ have opposite signs, as follows from the calculation data. This situation does not occur in the vicinity of $\lambda_{mag} = 813.42727$ nm [3] for the Sr atom, although in this case there is a similar range of opposite signs of $\Delta\beta^{circ}$ and $\Delta\beta^{lin}$ between the lattice nodes at λ = 800 and 803 nm, respectively, which are at a rather large distance from λ_{mag}, as shown in Fig. 2.

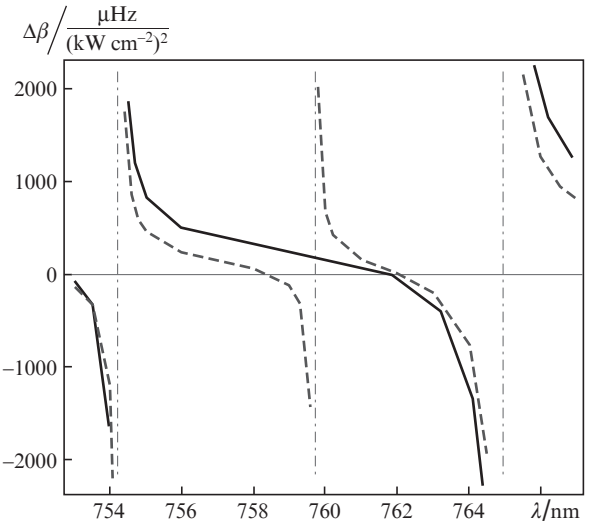

Figure 1. Dependences of the hyperpolarisability on the wavelength λ for a clock transition in Yb atoms at (dashed line) linear and (solid line) circular polarisations of the optical lattice laser wave. The vertical lines indicate the positions of two-photon resonances on the levels 6s8p(^{3}P$_2$) (λ = 754.226 nm), 6s8p(^{3}P$_0$) (λ = 759.71 nm; this resonance arises only in the case of linear polarisation) and 6s5f(^{3}F$_2$) (λ = 764.953 nm).

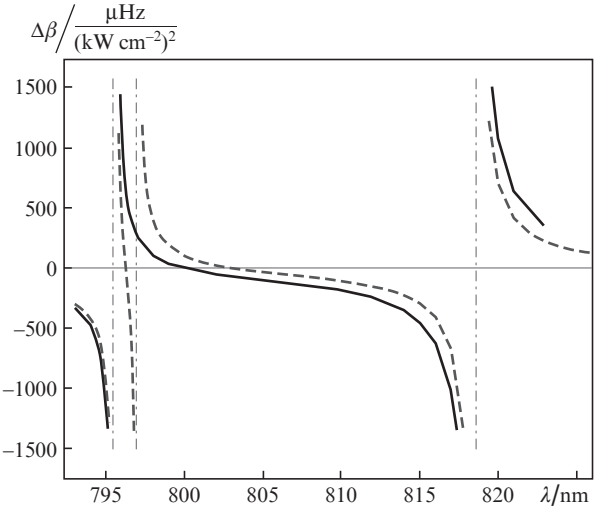

Figure 2. Dependences of the hyperpolarisability on the wavelength λ for a clock transition in Sr atoms at (dashed line) linear and (solid line) circular polarisations of the optical lattice laser wave. The vertical lines indicate the positions of two-photon resonances on the levels 5s7p(^{3}P$_2$) (λ = 795.5 nm), 5s7p(^{3}P$_0$) (λ = 797 nm; this resonance arises only in the case of linear polarisation), and 5s4f(^{3}F$_2$) (λ = 818.6 nm).

Note that, along with the frequency shift associated with the real part of hyperpolarisability $\Delta\beta^{lin(circ)}$, the excited states of clock transitions of Hg atoms at the MWL undergo a comparable (in amplitude) broadening, which is caused by the two-photon ionisation and described by the imaginary part of hyperpolarisability. The Im $\Delta\beta^{lin(circ)}$ value is positive for an arbitrary polarisation of the laser lattice field. The aforementioned effects are described by the coefficients c_i (except for the coefficient $c_{1/2}$, which does not contain any hyperpolarisability corrections), related to the imaginary part of the shift (17).

In contrast to Hg atoms, the imaginary part of hyperpolarisability for Sr atoms in the lattice at blue MWL detuning is three orders of magnitude smaller than the real part. Thus, the broadening of the clock transition line is negligible in comparison with the frequency shift in this case.

3. Strategies for determining the MWL in the case of red detuning

Obviously, the main contribution to the Stark energy (11) of a trapped atom at the laser field MWL is determined by the E1 polarisability, which exceeds the M1 and E2 polarisabilities by more than six orders of magnitude. Therefore, the difference in the MWLs found from formulas (1)–(3) may manifest itself only at the level of the sixth decimal place. Nevertheless, this difference may significantly affect the numerical values of the coefficients at laser field intensities in integer and fractional powers and, therefore, the frequency shift (17) of the clock transition. In this section, we will consider three different approaches to determining MWL and report the numerical values for all coefficients.

3.1. Equivalence of the clock level shifts in a travelling wave

The electric dipole (E1), electric quadrupole (E2) and magnetic dipole interactions of the atom with the travelling-wave field are synchronous. Therefore, the shift in the first order in the field intensity I is determined by the sum of polarisabilities $\alpha^{\Sigma}_{g(e)}(\omega)$. To exclude this shift, the field frequency is tuned to the magic frequency $\omega = \omega^{t}_{mag}$, for which condition (1) is satisfied. For this frequency, the depth of potential (8) and all coefficients in the right-hand side of Eqn (17) have nonzero values:

$$c^{t}_{1/2}(n) = -2\Delta\alpha^{qm}_{t}\sqrt{\mathcal{E}^{rec}_{t}/\alpha^{\Sigma}_{t}}\left(n+\frac{1}{2}\right),$$

$$c^{t}_{1}(\xi,n) = \Delta\alpha^{qm}_{t} - \frac{3\mathcal{E}^{rec}_{t}}{2\alpha^{\Sigma}_{t}}\Delta\beta_{t}(\xi)\left(n^2+n+\frac{1}{2}\right), \qquad (19)$$

$$c^{t}_{3/2}(\xi,n) = 2\Delta\beta_{t}(\xi)\sqrt{\mathcal{E}^{rec}_{t}/\alpha^{\Sigma}_{t}}\left(n+\frac{1}{2}\right), \quad c^{t}_{2}(\xi) = -\Delta\beta_{t}(\xi),$$

where the index t corresponds to the travelling wave. The corrections to the hyperpolarisability effects for the lowest vibrational levels with $n < 3$ are negligible at the intensities necessary to trap atoms. For example, using the numerical data of Table 1 for Hg atoms, one can write the frequency shift (in mHz) induced by the optical lattice (17) in the form

$$\begin{aligned}\Delta\nu^{t}_{cl}(n,\xi,I) = {} & -9.507(2n+1)I^{1/2} \\ & + [8.25 + (0.005 - 0.01\xi^2)(n^2+n+1/2)]I \\ & + (5.80\xi^2 - 2.88)\,10^{-3}(2n+1)I^{3/2} \\ & + (2.5 - 5.03\xi^2)\,10^{-3}I^2, \end{aligned} \qquad (20)$$

where the laser lattice intensity I is taken in kW cm^{-2}. For $I > 2$ kW cm^{-2}, the positive value of the correction linear in I is completely compensated for by the negative root term, and the main correction (20) to the shift is determined by the terms proportional to $I^{3/2}$ and I^2. Accurate to the third decimal place, the dependences of the coefficient at I on n and ξ are negligible [as follows from Fig. 3, which shows dependence (20) for the minimum value of vibrational state energy ($n = 0$)].

3.2. Equivalence of the clock level shifts in a standing wave

In the standing wave of the optical lattice, atoms are cooled to temperatures $T < \Omega/2 \approx \mathcal{E}^{rec}/k_B \approx 1$ μK, due to which atoms can be trapped with the minimum vibrational energy and the principal vibrational quantum number $n = 0$. The root term can be excluded when $\alpha^{dqm}_{g}(\omega^{s}_{mag}) = \alpha^{dqm}_{e}(\omega^{s}_{mag}) \equiv \alpha^{dqm}_{s}$. Under these conditions, $c^{s}_{1/2} = 0$ and

$$\Delta\nu^{s}_{cl}(\xi,n,I) = c^{s}_{1}(\xi,n)I + c^{s}_{3/2}(\xi,n)I^{3/2} + c^{s}_{2}(n)I^2, \qquad (21)$$

where

$$c^{s}_{1}(\xi,n) = -\Delta\alpha^{qm}_{s} - \frac{3\mathcal{E}^{rec}_{s}}{2\alpha^{dqm}_{s}}\Delta\beta_{s}(\xi)\left(n^2+n+\frac{1}{2}\right),$$

$$c^{s}_{3/2}(\xi,n) = 2\Delta\beta_{s}(\xi)\sqrt{\mathcal{E}^{rec}_{s}/\alpha^{dqm}_{s}}\left(n+\frac{1}{2}\right), \qquad (22)$$

$$c^{s}_{2}(\xi) = -\Delta\beta_{s}(\xi).$$

The index s corresponds to the standing wave. Accurate to the third decimal place, the shift (21) for Hg atoms can be written without the root dependence and with negative sign for the linear term. The corresponding dependence is plotted in Fig. 4. As in the case of the travelling wave, the main correction to the shift is determined by the term linear in I, which depends basically on the difference in multipole polarisabilities, $\Delta\alpha^{qm}_{s}$.

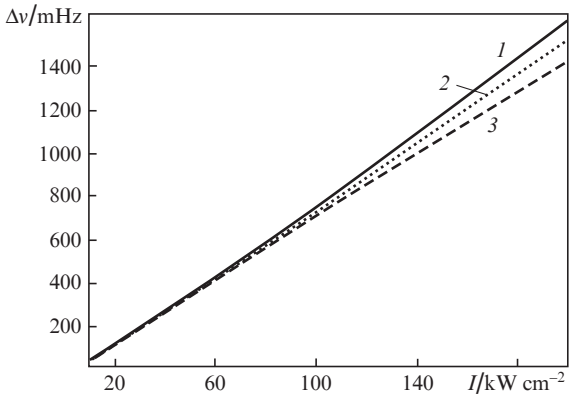

Figure 3. Dependences of the clock transition frequency shift $\Delta\nu$ in Hg atoms on the intensity I of the optical lattice with the MWL determined for a travelling wave. The frequency shifts correspond to (*1*) linear polarisation, (*2*) magic ellipticity and (*3*) circular polarisation.

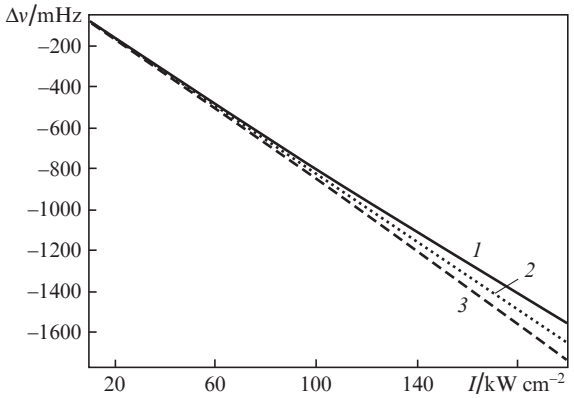

Figure 4. Dependences of the clock transition frequency shift $\Delta\nu$ in Hg atoms on the intensity I of the optical lattice with the MWL determined for a standing wave. The frequency shifts correspond to (*1*) linear polarisation, (*2*) magic ellipticity and (*3*) circular polarisation.

3.3. Equivalence of dipole polarisabilities for clock transitions

When $\alpha_g^{E1}(\omega_{mag}^{E1}) = \alpha_e^{E1}(\omega_{mag}^{E1}) \equiv \alpha_{mag}^{E1}$, the first-order corrections for the potential depth (8) are equivalent. Therefore, the main correction to the coefficient c_1, which is determined in (19) and (22) by the difference in multipole polarisabilities, $\Delta\alpha_{t(s)}^{qm}$, is compensated for, and the only correction that remains is the correction to hyperpolarisability, which is two orders of magnitude smaller (as follows from the data of Table 1). At the same time, the coefficient $c_{1/2}^{E1}$ is only half of the coefficient $c_{1/2}^{t}$ in Eqn (19). In this case, the coefficients in the right-hand side of Eqn (17) can be presented in the form

$$c_{1/2}^{E1}(n) = -\Delta\alpha_{mag}^{qm}\sqrt{\mathcal{E}_{E1}^{rec}/\alpha_{mag}^{E1}}\left(n+\frac{1}{2}\right),$$

$$c_1^{E1}(\xi,n) = -\frac{3\mathcal{E}_{E1}^{rec}}{2\alpha_{mag}^{E1}}\Delta\beta^{E1}(\xi)\left(n^2+n+\frac{1}{2}\right), \qquad (23)$$

$$c_{3/2}^{E1}(\xi,n) = 2\Delta\beta^{E1}(\xi)\sqrt{\mathcal{E}_{E1}^{rec}/\alpha_{mag}^{E1}}\left(n+\frac{1}{2}\right),$$

$$c_2^{E1}(\xi) = -\Delta\beta^{E1}(\xi).$$

Thus, in the case of equal dipole polarisabilities, the coefficients $c_1^{E1}(\xi,n)$, $c_{3/2}^{E1}(\xi,n)$, and $c_2^{E1}(\xi,n)$ are proportional to the difference in hyperpolarisabilities $\Delta\beta^{E1}(\xi)$.

Obviously, in all three above-described strategies for determining the MWL, the coefficients $c_{3/2}$ and c_2, coinciding accurate to the sixth decimal place, are proportional to $\Delta\beta(\xi)$. The coefficient at the root dependence is $c_{1/2}^{s} = 0$, whereas the MWL values determined by Eqns (1) and (3) are equivalent when the condition $c_{1/2}^{E1} \approx 0.5c_{1/2}^{t}$ is satisfied and proportional to the difference in multipole polarisabilities, $\Delta\alpha_{mag}^{qm}$. As follows from Table 1, the coefficients at the linear term in (17) satisfy the condition $|c_1^{E1}| \ll |c_1^{s}| \approx |c_1^{t}|$. The corrections for multipole interactions to the coefficients $c_1^{t}(\xi,n)$ and $c_1^{s}(\xi,n)$ have opposite signs, whereas the corrections for anharmonic interactions to the coefficient $c_1^{t(s)}(\xi,n)$ are proportional to $\Delta\beta(\xi)$, and this difference is much smaller than $\Delta\alpha_{mag}^{qm}$. Estimates show that, choosing the magic frequency ω_{mag}^{E1}, one can influence the contribution of the nonlinear and multipole shifts to the clock transition frequency and, therefore, minimise the error caused by the laser lattice effect. The dependence of the frequency shift (in mHz) (17) of the clock transition on the intensity, with the coefficients (23) for Hg atoms, can be presented numerically in the form

$$\Delta\nu_{cl}^{E1}(n,\xi,I) = -9.507(n+1/2)I^{1/2}$$
$$+ (4.98 - 10.02\xi^2)\,10^{-3}(n^2+n+1/2)]I$$
$$+ (5.80\xi^2 - 2.88)\,10^{-3}(n+1/2)I^{3/2}$$
$$+ (2.50 - 5.03\xi^2)\,10^{-3}I^2, \qquad (24)$$

where the intensity is in kW cm^{-2}. For the magic degree of circular polarisation $\xi_{mag} = \pm 0.705$, all hyperpolarisabilities (dependent on $-\xi$) in the right-hand sides of Eqns (23) and (24) are zero, and it is only the term with $I^{1/2}$ that remains nonzero. In this case, the only nonzero term is the non-excluded shift induced by the laser lattice; for the lowest vibrational level ($n = 0$), this shift is $\Delta\nu_{cl}^{E1}(0,\xi_{mag},I) = -4.75I^{1/2}$. Therefore, at $I = 25$ kW cm^{-2}, to increase the accuracy of measuring the clock transition frequency to the 18th decimal place, this shift must be controlled with an error smaller than 4% as a minimum. For the linear polarisation ($\xi = 0$), the shift is

$$\Delta\nu_{cl}^{E1}(0,0,I) = -4.75I^{1/2} + 2.49\times10^{-3}I$$
$$- 2.88\times10^{-3}I^{3/2} + 2.5\times10^{-3}I^2.$$

Here, the positive linear and quadratic corrections are completely compensated for at $I = 163$ kW cm^{-2}, as follows from Fig. 5, by the negative corrections proportional to $I^{1/2}$ and $I^{3/2}$.

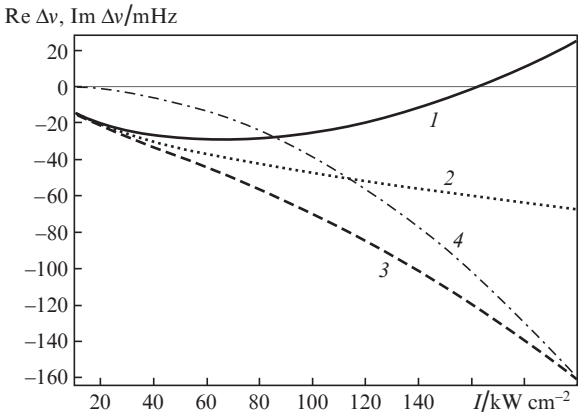

Figure 5. Dependences of the real part of the clock transition frequency shift $\Delta\nu$ in Hg atoms, trapped into the ground state with the vibrational quantum number $n = 0$, on the intensity I for the linear polarisation [$\xi = 0$; (*1*)], magic ellipticity [$\xi = \xi_{mag}$; (*2*)], and circular polarisation [$\xi = 1$; (*3*)] of the laser wave in the case of equivalent dipole polarisabilities for the MWL; curve (*4*) corresponds to the imaginary part of the frequency shift [broadening of the clock transition line (25)] for linearly polarised ($\xi = 0$) laser field.

The dependences of the frequency shifts induced by the laser lattice on the lattice field intensity are presented in Figs 3–5 for the clock transition in Hg atoms at $n = 0$ for three different MWLs: in a travelling wave (Fig. 3), in a standing wave (Fig. 4) and in the intermediate case of equal dipole polarisabilities (Fig. 5). As follows from these plots, for the MWLs determined in the cases of travelling and standing waves (Figs 3, 4), the frequency shift induced by the laser lattice depends weakly on the polarisation of the laser lattice field, because the hyperpolarisability contribution is negligible (in comparison with the corrections taking into account the multipole polarisabilities) in the intensity range $I < 200$ kW cm^{-2}. In contrast, in the case of equal dipole polarisabilities for the MWL (Fig. 5), where the corrections to the linear (in intensity) term that are related to the multipole polarisabilities are completely compensated for, and only the contributions from hyperpolarisabilities to the coefficients c_i ($i = 1, 3/2, 2$) condition the dependence of the frequency shift on the laser wave polarisation. Therefore, this case is most interesting for the clock transition spectroscopy. The hyperpolarisability correction depends strongly on the laser wave polarisation. In the case of linear polarisation ($\xi = 0$), at an intensity of $I \approx 160$ kW cm^{-2}, the positive corrections introduced by the linear and quadratic (in intensity I) terms of equation (17) can be compensated for by the negative corrections, which are proportional to $I^{1/2}$ and $I^{3/2}$. For circular and elliptical polarisations with $\xi > \xi_{mag} \approx 0.7$, the hyper-

Table 2. Coefficients for the laser-lattice-induced frequency shift (17) in the case of vibrational levels with $n = 0$.

Atom	$c^{t}_{1/2} = 2c^{E1}_{1/2}$/ mHz/$\sqrt{\text{kW cm}^{-2}}$	$c^{s}_{1/2}$/ mHz/$\sqrt{\text{kW cm}^{-2}}$	$c^{t}_{1} = -c^{s}_{1}$/ mHz/$\sqrt{\text{kW cm}^{-2}}$	$c^{E1}_{1}(\xi = 0)$/ mHz/$\sqrt{\text{kW cm}^{-2}}$	$c^{E1}_{1}(\xi = \pm 1)$/ mHz/$\sqrt{\text{kW cm}^{-2}}$	$c^{t(s,E1)}_{3/2}(\xi = 0)$/ mHz/$\sqrt{\text{kW cm}^{-2}}$	$c^{t(s,E1)}_{3/2}(\xi = \pm 1)$/ mHz/$(\text{kW cm}^{-2})^{3/2}$	$c^{t(s,E1)}_{2}(\xi = 0)$/ mHz/$(\text{kW cm}^{-2})^{2}$	$c^{t(s,E1)}_{2}(\xi = \pm 1)$/ mHz/$(\text{kW cm}^{-2})^{2}$
Sr	−0.382	0	1.39	0.0115	0.0179	−0.0554	−0.0862	0.200	0.311
Yb	1.79	0	−8.06	0.0136	−0.0089	−0.0814	0.0534	0.366	−0.240
Hg	−9.51	0	8.25	0.0025	−0.0025	−0.0029	0.0029	−0.240	−0.00253

polarisability corrections for the frequency shift are negative and increase with increasing intensity I (Fig. 5).

Thus, the fundamental feature of mercury atoms in an optical lattice with the MWL for equivalent dipole polarisabilities is the possibility of controlling with high efficiency the lattice-induced frequency shift (24) by changing the intensity and polarisation. An appropriate choice of I and ξ ($\xi < \xi_{\text{mag}}$) makes it possible to exclude this shift. However, one must also take into account the imaginary part $\Delta\nu^{E1}_{\text{cl}}(n,\xi,I)$, which corresponds to the two-photon ionisation of the upper clock transition level in the laser-wave field of the optical lattice. For example, in addition to the shift caused by the real part of hyperpolarisability, there is an effect of ionisation broadening $\Gamma(\xi,n,I) = \text{Im}\,\Delta\nu(\xi,n,I)$ of the clock transition line in mercury atoms at the MWL; this broadening is determined by the imaginary part of hyperpolarisability:

$$\Gamma(\xi,n,I) = \text{Im}\,[c_1(\xi,n)]I + \text{Im}\,[c_{3/2}(\xi,n)]I^{3/2} + \text{Im}\,[c_2(\xi,n)]I^2 = \text{Im}\,\Delta\beta(\xi)\left[-\frac{3\mathcal{E}^{\text{rec}}}{2\alpha_{\text{mag}}}\left(n^2 + n + \frac{1}{2}\right)I + \sqrt{\mathcal{E}^{\text{rec}}/\alpha_{\text{mag}}}\,(2n+1)I^{3/2} - I^2\right]. \quad (25)$$

As was noted above, this broadening gives rise to an additional error, related to the two-photon ionisation; it must be taken into account when estimating the error of an optical frequency standard based on laser lattice. Figure 5 shows the dependences for the real and imaginary components of the frequency shift (17) at $n = 0$ and $\xi = 0$.

Figures 6 and 7 show the most interesting dependences of the frequency shifts $\Delta\nu^{s}_{\text{cl}}(0,\xi,I)$ for Sr atoms and $\Delta\nu^{E1}_{\text{cl}}(0,\xi,I)$ for Yb atoms. In accordance with Eqns (19)–(23), the numerical

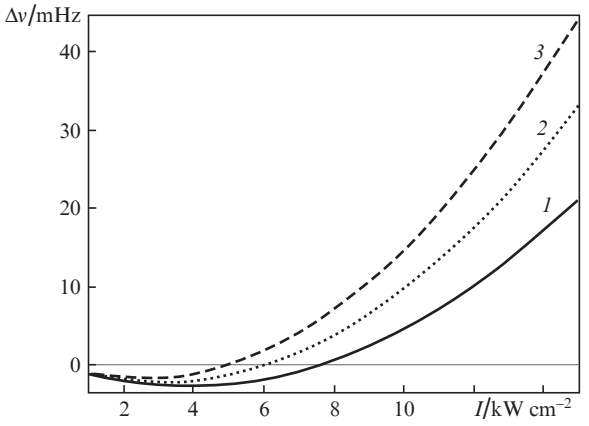

Figure 6. Dependences of the clock transition frequency shift $\Delta\nu$ in Sr atoms on the intensity I in the cases of (*1*) linear, (*2*) elliptical and (*3*) circular polarisations for the optical lattice MWL (case of laser field standing wave).

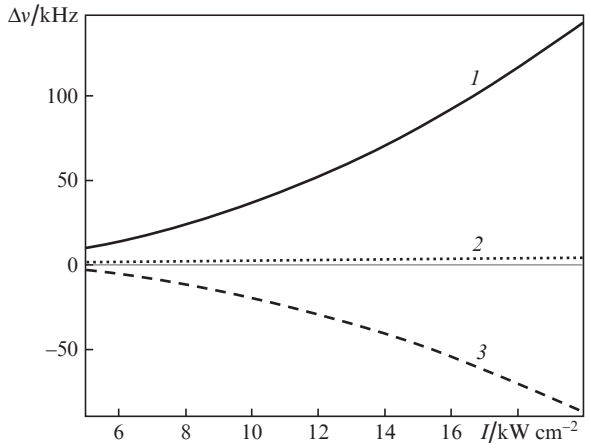

Figure 7. Dependences of the clock transition frequency shift $\Delta\nu$ in Yb atoms on the intensity I for the (*1*) linear, (*2*) elliptical and (*3*) circular polarisations of the optical lattice; the MWL was determined for equivalent dipole polarisabilities.

values of coefficients c_i (i = 1/2, 1, 3/2, 2) are listed in Table 2. The negative values of the corrections for the terms in (17) that are proportional to $I^{1/2}$ and $I^{3/2}$, for Sr atoms in the laser lattice at the MWL (the case of standing wave), are compensated for by the positive corrections for the terms proportional to I^2, even at intensities from 5 kW cm^{-2} (circular polarisation) to 8 kW cm^{-2} (linear polarisation), and the dependence $\Delta\nu^{s}_{\text{cl}}(n = 0,\xi,I)$ is transformed into a parabola with a positive leading coefficient $c^{s}_{2}(\xi) = 0.2 + 0.111\xi^2$ mHz (kW cm^{-2})$^{-2}$ (Fig. 6).

A more interesting result may occur for the shift $\Delta\nu^{E1}_{\text{cl}}(n = 0, \xi = \xi_{\text{mag}}, I)$ in Yb atoms (Fig. 7), for which $c^{E1}_{1}(\xi_{\text{mag}}) = c^{E1}_{3/2}(\xi_{\text{mag}}) = c^{E1}_{2}(\xi_{\text{mag}}) = 0$. In general, for the range of intensities I under consideration, the shift may be reduced practically to zero using the corresponding degrees of circular polarisation ξ_{mag}: $\Delta\nu^{E1}_{\text{cl}}(n = 0,\xi_{\text{mag}},I) = 0$. In particular, $\xi^2_{\text{mag}}(I =$ 5 kW cm^{-2}) ≈ 0.314, $\xi^2_{\text{mag}}(I =$ 10 kW cm^{-2}) ≈ 0.504, and $\lim\limits_{I\to\infty}\xi^2_{\text{mag}} \to 0.6044$.

4. Blue-detuned MWL

In the case of the MWL for an optical lattice with a repulsive potential, the corresponding values of the dipole polarisability are negative, $\alpha^{E1}_{g(e)}(\omega) < 0$, while the Stark energy is positive; therefore, the atomic equilibrium positions are near the nodes of lattice standing wave with the electric field

$$\boldsymbol{E}(X,t) = 2\boldsymbol{E}_0 \sin(kX)\sin(\omega t). \quad (26)$$

The spatial part of the interaction operator between the atom and lattice field (26) can be described by the expression

$$\hat{V}(X) = \hat{V}_{E1}\sin(kX) + (\hat{V}_{E2} + \hat{V}_{M1})\cos(kX) \quad (27)$$

with the operators of E1, E2 and M1 interactions in form (6). The trapping potential of the optical lattice with the MWL, which takes into account the dependence on the hyperpolarisability and anharmonicity effects, may be presented, similarly to the case of the MWL with red detuning, in form (7). The main advantage of the repulsive potential is that the localisation domain of atoms is in the vicinity of the nodes of the lattice standing wave; the field in these nodes becomes zero. Therefore, hyperpolarisability effects cannot arise in the regions of minimum potential energy and, correspondingly, affect the eigenfrequencies of vibrational levels:

$$U^{(0)}_{\mathrm{g(e)}}(I) \equiv U^{\mathrm{latt}}_{\mathrm{g(e)}}(X=0,I) = -\alpha^{\mathrm{qm}}_{\mathrm{g(e)}}(\omega)I,$$
$$\Omega_{\mathrm{g(e)}} = 2\sqrt{-\mathcal{E}^{\mathrm{rec}}\alpha^{\mathrm{dqm}}_{\mathrm{g(e)}}(\omega)I}. \qquad (28)$$

The energies of atomic vibrational levels near the nodes of a standing wave with MWL under conditions of blue detuning are given by the expression

$$\mathcal{E}^{\mathrm{vib}}_{\mathrm{g(e)}}(I,n) = U^{(0)}_{\mathrm{g(e)}} + \Omega_{\mathrm{g(e)}}\left(n+\frac{1}{2}\right) - \mathcal{E}^{\mathrm{anh}}_{\mathrm{g(e)}}(I)\left(n^2+n+\frac{1}{2}\right), \quad (29)$$

in which the hyperpolarisability effects can be taken into account only in the anharmonic correction

$$\mathcal{E}^{\mathrm{anh}}_{\mathrm{g(e)}}(I) = \frac{1}{2}\mathcal{E}^{\mathrm{rec}}\left[1-\frac{3\beta_{\mathrm{g(e)}}(\omega)I}{\alpha^{\mathrm{dqm}}_{\mathrm{g(e)}}(\omega)}\right], \quad (30)$$

which contains, in addition to (29), a correction in the form

$$\Delta\nu^{\mathrm{latt}}_{\mathrm{cl}}(\omega_{\mathrm{mag}},I,n) = \mathcal{E}^{\mathrm{vib}}_{\mathrm{e}} - \mathcal{E}^{\mathrm{vib}}_{\mathrm{g}} = c_{1/2}(n)I^{1/2} + c_1(n)I, \quad (31)$$

where

$$c_{1/2}(n) = \sqrt{\mathcal{E}^{\mathrm{rec}}}\left(\sqrt{-\alpha^{\mathrm{dqm}}_{\mathrm{e}}(\omega_{\mathrm{mag}})} - \sqrt{-\alpha^{\mathrm{dqm}}_{\mathrm{g}}(\omega_{\mathrm{mag}})}\right)(2n+1);$$

$$c_1(n) = -\Delta\alpha^{\mathrm{qm}}(\omega_{\mathrm{mag}}) \qquad (32)$$
$$+\frac{2\mathcal{E}^{\mathrm{rec}}}{2}\left[\frac{\beta_{\mathrm{e}}(\omega_{\mathrm{mag}})}{\alpha^{\mathrm{dqm}}_{\mathrm{e}}(\omega_{\mathrm{mag}})} - \frac{\beta_{\mathrm{g}}(\omega_{\mathrm{mag}})}{\alpha^{\mathrm{dqm}}_{\mathrm{g}}(\omega_{\mathrm{mag}})}\right]\left(n^2+n+\frac{1}{2}\right).$$

The main correction to the lattice-field-induced frequency shift of the optical transition is described by the second term in the right-hand side of Eqn (29). Therefore, the choice of the MWL implies provision of equivalence conditions for the vibrational eigenfrequencies (28), characterised by a root dependence on the laser field intensity, of atoms in the ground and excited states: $\Omega_{\mathrm{g}} = \Omega_{\mathrm{e}}$. This means that, at this choice of the MWL, the coefficient $c_{1/2}(n)$ may turn to zero, as a result of which only a linear dependence on I remains in expression (31). The linear frequency shift is 136 mHz at I = 10 kW cm^{-2} (see Table 1); therefore, one must carefully control it when carrying out high-precision measurements of clock transition frequency.

5. Use of the model potential method for calculating the electromagnetic polarisabilities of alkaline-earth atoms

The MWL calculations in the single-electron approximation of the model potential [7], using the corresponding empirical parameters determined from the known energies of atomic levels [12], provide numerical data for the Sr, Yb and Hg atoms, close to the experimental values known from the literature (see the data on λ_{mag} in Table 1). The calculation results are presented in Figs 8–10.

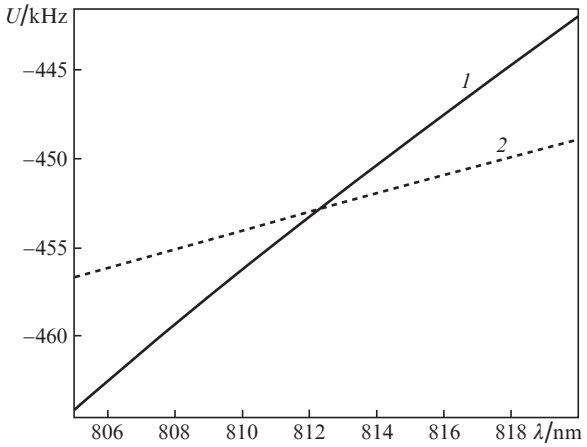

Figure 8. Wavelength dependences of the lattice potential depth U at a laser field intensity I = 10 kW cm^{-2} for Sr atoms in the (*1*) excited ($5s5p\,^3P_0$) and (*2*) ground ($5s^2\,^1S_0$) states.

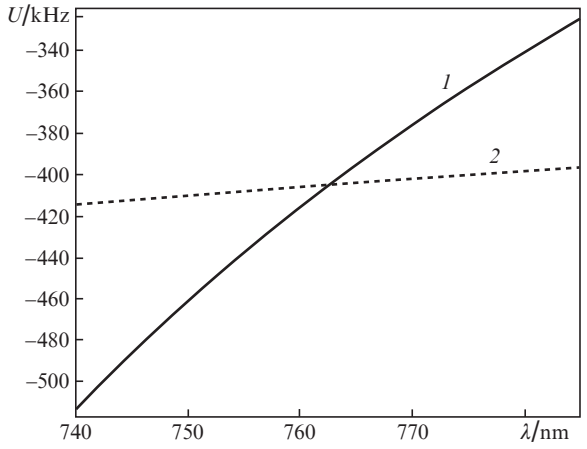

Figure 9. Wavelength dependences of the lattice potential depth U at a laser field intensity I = 10 kW cm^{-2} for Yb atoms in the (*1*) excited ($6s6p\,^3P_0$) and (*2*) ground ($6s^2\,^1S_0$) states. The results of the calculation in the model potential approximation ($\lambda_{\mathrm{mag}} \approx 762.6$ nm) are in good agreement with the experimental data ($\lambda^{\mathrm{exp}}_{\mathrm{mag}} \approx 759.3537$ nm [4]).

In general, the methods for calculating the spectroscopic characteristics of a many-electron atom using the single-electron approximation require some modification of the FMP method, more specifically, the choice of its parameters. This modification was demonstrated for the first time in [13]; then this approach was successfully used in the calculations of polarisabilities, hyperpolarisabilities, interactions of atoms with external fields, dynamic interactions, etc. (see, e.g., [7, 14–17]).

The basic concept of this modification is as follows. First of all, we introduce fractional values for the orbital momentum of triplet S states $\tilde{l}_{^3\mathrm{S}}$, which, nevertheless, must be close to the real orbital momenta of S states ($\tilde{l}_{^3\mathrm{S}} \approx l_{\mathrm{S}} = 0$), and effective momenta for the singlet and triplet D states, which must satisfy

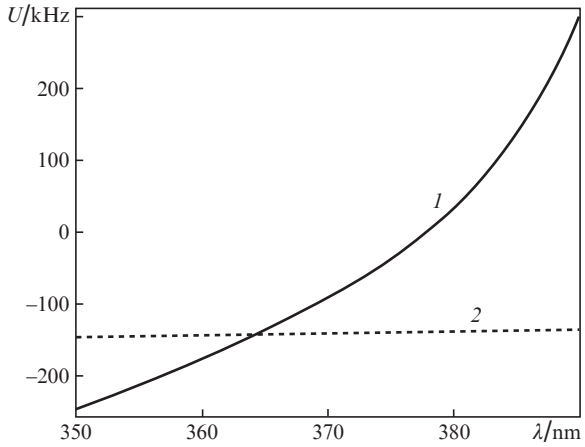

Figure 10. Wavelength dependences of the lattice potential depth U at a laser field intensity $I = 25$ kW cm^{-2} for Hg atoms in the (*1*) excited ($6s6p\,^3P_0$) and (*2*) ground ($6s^2\,^1S_0$) states. The results of the calculation in the model potential approximation ($\lambda_{mag} \approx 364$ nm) are in good agreement with the experimental data ($\lambda_{mag}^{exp} \approx 362.53$ nm [5]).

the equality $\tilde{l}_{^3D} \approx \tilde{l}_{^1D} \approx l_D = 2$. This choice leads to redetermination of the integer values for the radial quantum number n_r in order to provide the initial equality $\tilde{l}_{^3S} + n_r + 1 = \nu_{nl}$ for the effective principal quantum number ν_{nl}, which is found from the energy $\mathcal{E}_{nl} = -Z^2/(2\nu_{nl}^2)$ of the atomic state $|nl\rangle$ (Z is the effective nucleus charge).

The above-considered modification of the FMP method was used in this study in the calculations of the entire set of characteristics of Sr, Yb and Hg atoms.

6. Conclusions

We performed precise calculations of the higher-order nonlinear optical effects occurring in the interaction of alkaline-earth atoms with the optical lattice field in order to analyse the possible use of the potential of these atoms in modern optical frequency standards based on optical lattices. In particular, the multipole expansions of the interaction operator between the atoms and lattice field for the electric dipole (E1) and multipole (M1 and E2) interactions were considered. Algorithms for calculating the MWL values for the red and blue detunings of the laser lattice field were elaborated analytically and numerically. The requirements to the accuracy of determining MWL in different strategies of measuring the clock transition frequencies for the Sr, Yb and Hg atoms in an optical lattice were formulated. It was shown that, in some situations, the contributions of nonlinear optical higher-order effects cannot be compensated for by the choice of the MWL; therefore, they must be correctly taken into account when analysing the results of measuring the clock transition frequency in optical frequency standards [18, 19].

Acknowledgements. This work was supported in part by the Ministry of Education and Science of the Russian Foundation (Project Nos 3.7514.2017/8.9 and 3.1659.2017/8.6).

References

1. Chou C.W., Hume D.B., Koelemeij J.C.J., Wineland D.J., Rosenband T. *Phys. Rev. Lett.*, **104**, 070802 (2010).
2. Nemitz N., Ohkubo T., Takamoto M., Ushijima I., Das M., Ohmae N., Katori H. *Nat. Photonics*, **10**, 258 (2016).
3. Westergaard P.G., Lodewyck J., Lorini L., Lecallier A., Burt E.A., Zawada M., Millo J., Lemonde P. *Phys. Rev. Lett.*, **106**, 210801 (2011).
4. Barber Z.W., Stalnaker J.E., Lemke N.D., et al. *Phys. Rev. Lett.*, **100**, 103002 (2008).
5. Mejri S., Yi L., McFerran J.J., Le Coq Y., Bize S. *Phys. Rev. Lett.*, **106**, 073005 (2011).
6. Ovsiannikov V.D., Pal'chikov V.G., Taichenachev A.V., Yudin V.I., Katori H. *Phys. Rev. A*, **88**, 013405 (2013).
7. Manakov N.L., Ovsiannikov V.D., Rapoport L.P. *Phys. Rep.*, **141**, 319 (1986).
8. Katori H., Takamoto M., Pal'chikov V.G., Ovsiannikov V.D. *Phys. Rev. Lett.*, **91**, 173005 (2003).
9. Taichenachev A.V., Yudin V.I., Ovsiannikov V.D., Pal'chikov V.G., Oates C.W. *Phys. Rev. Lett.*, **101**, 193601 (2008).
10. Taichenachev A.V., Yudin V.I., Ovsiannikov V.D., Pal'chikov V.G. *Phys. Rev. Lett.*, **97**, 173601 (2006).
11. Takamoto M., Katori H., Marmo S.I., Ovsiannikov V.D., Pal'chikov V.G. *Phys. Rev. Lett.*, **102**, 063002 (2009).
12. NIST Atomic Spectra Database: http://physics.nist.gov/asd.
13. Simons G. *J. Chem. Phys.*, **55**, 756 (1971).
14. Kostelecky V.A., Nieto M.M. *Phys. Rev. A*, **32**, 3243 (1985).
15. Djerad M.T. *J. Phys. II*, **1**, 1 (1991).
16. Celik G., Ates S., Ozarslan S., Taser M. *J. Quant. Spectrosc. Radiat. Transfer*, **112**, 2330 (2011).
17. Katori H., Ovsiannikov V.D., Marmo S.I., Palchikov V.G. *Phys. Rev. A*, **91**, 052503 (2015).
18. Ovsiannikov V.D., Marmo S.I., Palchikov V.G., Katori H. *Phys. Rev. A*, **93**, 043420 (2016).
19. Schioppo M., Brown R.C., McGrew W.F., Hinkley N., Fasano R.J., Beloy K., Yoon T.H., Milani G., Nicolodi D., Sherman J.A., Phillips N.B., Oates C.W., Ludlow A.D. *Nat. Photonics*, **11**, 48 (2017).